JCTC Journal of Chemical Theory and Computation

Article

pubs.acs.org/JCTC

Accurate, Precise, and Efficient Theoretical Methods To Calculate Anion−π Interaction Energies in Model Structures

Pál D. Mezei,[†] Gábor I. Csonka,*[,†] Adrienn Ruzsinszky,[‡] and Jianwei Sun[‡]

[†]Department of Inorganic and Analytical Chemistry, Budapest University of Technology and Economics, H-1521 Budapest, Hungary

[‡]Department of Physics, Temple University, Philadelphia, Pennsylvania 19122, United States

Supporting Information

ABSTRACT: A correct description of the anion−π interaction is essential for the design of selective anion receptors and channels and important for advances in the field of supramolecular chemistry. However, it is challenging to do accurate, precise, and efficient calculations of this interaction, which are lacking in the literature. In this article, by testing sets of 20 binary anion−π complexes of fluoride, chloride, bromide, nitrate, or carbonate ions with hexafluorobenzene, 1,3,5-trifluorobenzene, 2,4,6-trifluoro-1,3,5-triazine, or 1,3,5-triazine and 30 ternary π−anion−π' sandwich complexes composed from the same monomers, we suggest domain-based local-pair natural orbital coupled cluster energies extrapolated to the complete basis-set limit as reference values. We give a detailed explanation of the origin of anion−π interactions, using the permanent quadrupole moments, static dipole polarizabilities, and electrostatic potential maps. We use symmetry-adapted perturbation theory (SAPT) to calculate the components of the anion−π interaction energies. We examine the performance of the direct random phase approximation (dRPA), the second-order screened exchange (SOSEX), local-pair natural-orbital (LPNO) coupled electron pair approximation (CEPA), and several dispersion-corrected density functionals (including generalized gradient approximation (GGA), meta-GGA, and double hybrid density functional). The LPNO-CEPA/1 results show the best agreement with the reference results. The dRPA method is only slightly less accurate and precise than the LPNO-CEPA/1, but it is considerably more efficient (6−17 times faster) for the binary complexes studied in this paper. For 30 ternary π−anion−π' sandwich complexes, we give dRPA interaction energies as reference values. The double hybrid functionals are much more efficient but less accurate and precise than dRPA. The dispersion-corrected double hybrid PWPB95−D3(BJ) and B2PLYP−D3(BJ) functionals perform better than the GGA and meta-GGA functionals for the present test set.

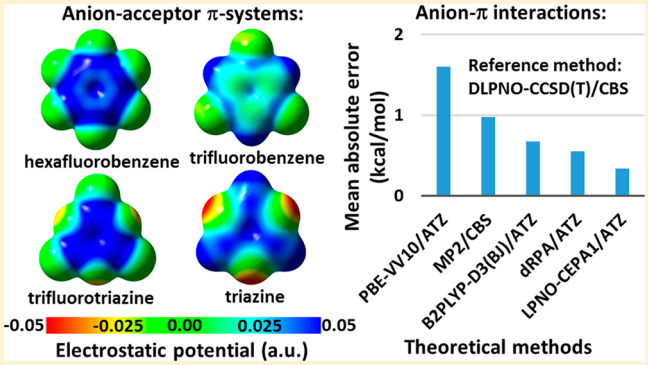

INTRODUCTION

Accurate description of noncovalent interactions is essential for further developments in self-assembly of molecules, catalysis, materials science, medicine, biological functions, and systems biology.[1−4] Noncovalent interactions of aromatic rings play a very important role in biology and chemistry,[5] for example in protein folding, drug−receptor interactions, crystal engineering, DNA and RNA stacking, protein DNA aromatic interactions, DNA repair, and maintaining DNA stability.[6]

The importance of cation−π interactions was recognized some time ago,[7−9] and an accurate description of preferred arrangements is quite feasible. Cation−π complexes can be described by a single type of minimum energy structure: the cation positions itself close to the ring center. The analogous structure to the cation−π complex, the anion−π complex, was ignored for a long time due to the supposed electrostatic repulsion.[10] However, recently this relatively unexplored interaction has gained attention.[11,12] A survey showed[13] that contrary to general expectations, anion−π interactions are more frequent in the Cambridge Structural Database[14] than cation−π interactions. Recently direct evidence for the anion−π interactions is obtained by tandem mass spectrometric experiments with naphthalenediimide models where only the π-acidic surface is left for anions to interact with.[15] The correct description of the interaction between anions and aromatic rings can be used for the design of selective anion receptors and channels, and this is important for the advances in the field of supramolecular chemistry.[16,17] For complexes with the fluoride ion a covalently bonded structure, called the "Meisenheimer" complex, is the most stable in gas phase.[18] A typical example is the 1,3,5-triazine (TAZ)···F^- complex. However, adding two water molecules to this complex makes the H-bonded complex more stable, competing with anion−π and displaced anion−π complex forms. Adding three or four water or acetonitrile molecules makes the displaced anion−π complex form the most stable.[18] Adding three or four water molecules to the TAZ···Cl^- complex makes the anion−π complex form the most

Received: September 11, 2014

   dx.doi.org/10.1021/ct5008263 | J. Chem. Theory Comput. XXXX, XXX, XXX−XXX

stable.[18] Since the anion−π and displaced anion−π forms are almost equally stable, these two forms occur in many crystal structures.[18] Compared to cation−π, the anion−π complex interaction energy is supposed to have a more significant van der Waals (vdW) and induction components, because anions have extended, polarizable electron clouds.[12]

In this work we focus on a quantitatively accurate and precise description of the anion−π complexes. We give high quality interaction energy values for benchmarks and analyze quantitatively the importance of the exchange, induction, electrostatic, and vdW energy components of the interaction energy. In the following section we provide the computational details. Next we analyze the performance of various dispersion-corrected density functionals up to double hybrids, dRPA and RPA, and give a cost performance evaluation. Finally we select the most efficient best-performing method for further studies.

METHODOLOGY

The vdW interaction is a universal noncovalent long-range attraction between chemical species, arising from a correlation between instantaneous electronic charge fluctuations on each. In the large separation limit of two ground-state spherical interacting atoms, the nonretarded potential energy of the vdW interaction between them can be expressed as a power series in the inverse of d. According to second-order perturbation theory at long-range we get a multipolar expansion

$$E_{vdW} = -\frac{C_6}{d^6} - \frac{C_8}{d^8} - \frac{C_{10}}{d^{10}} + \dots \quad (1)$$

where d is the internuclear separation (d must be sufficiently large to obtain nonoverlapping electron densities), the system-dependent C_6 describes the dynamic dipole−dipole interaction, C_8 describes the dipole−quadrupole interaction, and C_{10} describes the quadrupole−quadrupole and the dipole−octupole interactions. Even in the ground state, each sphere has a zero-point motion. The zero-point oscillations of the charge density in one sphere produce a long-range multipolar electric field that interacts with and correlates with the zero-point oscillations of the charge density in the other sphere. The vdW interaction is much weaker in strength than a usual chemical bond, but a correct description of such weak interactions might be critical for biological or material science applications. Long- and medium-ranged weak interactions are largely responsible for many phenomena such as sublimation of molecular solids, high interlayer mobility of graphite, folding of long biomolecular chains such as DNA, RNA, and proteins, folding of polymers, and many others.

The wave function based methods that include electron correlation effects, such as configuration interaction (CI), many-body perturbation theory (MBPT), or coupled cluster (CC) methods, are able to estimate vdW interaction energy quite reasonably. The CC singles and doubles with perturbative triples, CCSD(T), method is currently the reference method for noncovalent interactions, but its applicability is limited to single-reference ground states and to relatively small systems due to its steep N^7 scaling of computational cost with system size N. This method shows slow basis set convergence and expensive basis set extrapolations are necessary for useful precision, but notice the emerging new localized CC methods that efficiently decrease the computational time and scaling with size.[19] The much less expensive second-order direct Møller−Plesset perturbation theory (MP2) includes long-range interactions but leads to mixed results for anion−π complex interaction energy.

A relatively inexpensive but usefully accurate method can be constructed based on density functional theory (DFT).[20−24] The asymptotic interaction energy of semilocal DFT approximations decreases exponentially instead of the proper minus sixth power. This failure greatly limits the applicability of pure semilocal DFT to a large class of weakly bound systems such as atom and intermolecular pairs, liquids, and molecular crystals. To overcome or reduce this error, a dispersion correction can be added in a "post-Kohn-Sham manner" by pairwise interactions.[25] Pair-wise interaction can be constructed in empirical[26] or nonempirical ways.[27] In the latter approach, a nonempirical model is proposed for the multipole polarizability or C_{2k} coefficients based on physical constraints. Grimme et al. introduced the D3 model[28] that uses precomputed dispersion coefficients, and the environment of an atom in a molecule is modeled by a fractional coordination number. D3(BJ)[29] is an improved variant of D3 that uses the damping of Becke and Johnson (BJ).[30]

An alternative strategy is to add approximate dispersion energy via MP2 or Görling-Levy second-order Kohn−Sham perturbation theory.[31,32] This is the basic idea behind the so-called double hybrid methods that combine semilocal DFT functionals, exact exchange, and second order perturbation theory reviewed in ref 26. Notice that double hybrid functionals miss a considerable part of long-range correlation effects and require *a posteriori* dispersion correction for better results.[29]

Interesting alternatives are the nonlocal vdW correlation functionals that model the multipole polarizability. Unlike the pairwise approaches, which usually take the static polarizability as an input from experiment or higher-level calculation, the nonlocal correlation approximations are functionals of the density, making a seamless approximation for the nonlocal correlation energy. Long-range van der Waals functionals of the Langreth[33−35] or Vydrov-van Voorhis-type (VV10)[36] start from a semilocal exchange-correlation functional and then add a fully nonlocal correction. Thus, these methods strongly rely upon the underlying semilocal approximation.

Most approximations, including the pairwise models and the nonlocal van der Waals functionals as well, miss the many-body terms arising from the coupling of the oscillators. The number of atoms is additive, but the exact multipole polarizability is not. The exact multipole polarizability is also nonlocal. The direct Random Phase Approximation (dRPA) using the Kohn−Sham orbitals and orbital energies[37−39] provides a "seamless" treatment of all forces including vdW at any separation. dRPA neglects antisymmetrization effects on the correlation energy that are included in full RPA. The correlation energy in the dRPA can be understood as the zero-point vibrational energy of virtual electronic transitions. dRPA contains the zero-point energy of plasmons coupled by the long-ranged Coulomb interaction between subsystems. Its long-range correlation is almost exact, and it properly captures the nonpairwise-additive nature of long-range interactions.[40−42] Notice that dRPA is exact for the exchange energy but not for the correlation energy. It can also be derived from the "ring-coupled cluster" theory by removal of the exchange terms from the two-particle Hamiltonian.[43] The absence of these terms is responsible for a self-correlation error and for the expected failure of the dRPA for stretched H_2^+, He_2^+, and Ne_2^+.[44−46] We have argued that the RPA correlation hole, even after semilocal or short-range correction, is not correct at midrange in a molecule.[47,48] This is

dx.doi.org/10.1021/ct5008263 | J. Chem. Theory Comput. XXXX, XXX, XXX−XXX

an interesting complementarity to semilocal DFT, where the short- and midrange energy might be correct but not the long-range component of the energy.

COMPUTATIONAL DETAILS

We investigate 20 binary anion−π complexes of fluoride, chloride, bromide, nitrate, or carbonate ions with hexafluorobenzene (HFB), 1,3,5-trifluorobenzene (TFB), 2,4,6-trifluoro-1,3,5-triazine (TFZ), or 1,3,5-triazine (TAZ) as shown in Figure 1 and 30 ternary π−anion−π' sandwich complexes as shown in Figure 2.[1]

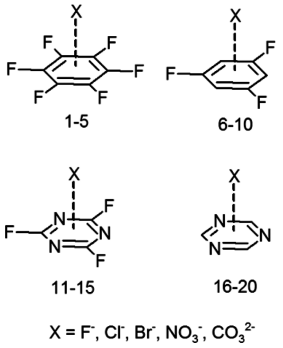

Figure 1. Structure and the main symmetry axis of the anion−π binary complexes 1−20 taken from ref 1.

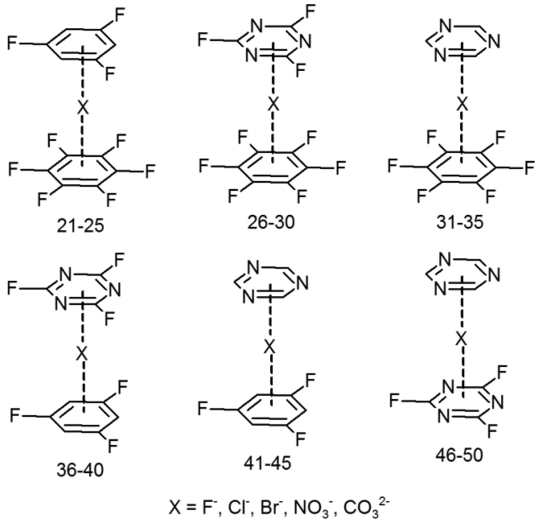

Figure 2. Structure and the main symmetry axis of the π−anion−π' ternary complexes 21−50 taken from ref 1.

The resolution of the identity MP2 (RI-MP2) method is considerably faster than the MP2, and it was shown that the interaction energies and equilibrium distances are almost identical for both methods for HFB with anions, TFB with cations and anions, and TAZ with cations and anions.[49] Consequently the RI-MP2 method can replace the MP2 for the calculations of ion-π interactions.[49] The RI-MP2/6-31++G-(d,p) equilibrium molecular geometries of the monomers and the 20 anion−π and 30 sandwich complexes were taken from the literature.[1] We did not use the alternatively available MPWB1K/6-31++G(d,p) optimized geometries[1] as those yield higher CCSD(T) energies and are thus less optimal for our purposes. The application of different geometries results in a 1−2 kcal mol^{-1} energy change.

The DFT calculations were performed by using Orca 3.0.1[50] on Intel Core i7-2630QM Processor. At the generalized gradient approximation (GGA) level we used the Perdew−Burke−Ernzerhof functional (PBE),[51] its revised version with more repulsive exchange (revPBE),[52] and the refitted Perdew−Wang 1986 exchange functional (rPW86) with the PBE correlation (rPWPBE).[53] At the meta-GGA level we used the Tao-Perdew-Staroverov-Scuseria functional (TPSS).[54] We also used three double hybrid functionals: 1) the B2PLYP[55] containing Becke 1988 exchange (B88),[56] exact exchange, Lee−Yang−Parr correlation (LYP),[57] and second order perturbation theory correlation (PT2); 2) the mPW2PLYP[58] containing modified Perdew−Wang 1991 exchange (mPW91),[59] exact exchange, and LYP and PT2 correlation terms; and 3) the PWPB95[60] containing the reparametrized version of PW91[61] exchange and B95[62] correlation functionals and also exact exchange and PT2 correlation. To accelerate the calculations, we applied the RI[63] approximation for the Coulomb, for the exact exchange and for the PT2 correlation terms (RI-J, RI-JK, and RI-C algorithms, respectively). The DF-BLYP and B3LYP results are poor for these complexes, and the interested readers might find those results in ref 49.

We used the MRCC[64] (06/20/2014 release) program for the density-fitted MP2, the random phase approximation with exchange terms (RPAx), direct RPA (dRPA) and dRPA + second order screened exchange (SOSEX) calculations.[65] The dRPA correlation energy is obtained as

$$E_c^{dRPA} = \frac{1}{2}\mathrm{tr}[\boldsymbol{BT}] \tag{2}$$

where $B_{ia,jb} = \langle ij|ab\rangle$ are nonantisymmetrized two electron repulsion integrals using occupied i,j and virtual a,b spin−orbital indices, and $T_{ia,jb} = t_{ij}^{ab}$ are the double excitation amplitude matrix elements. The amplitude matrix can be obtained from the solution of the Riccati equation as described in refs 43 and 66. This algorithm scales as $(N_{occ}N_{virt})^3$, where N_{occ} and N_{virt} are the number of occupied and unoccupied orbitals, respectively, leading to overall scaling of N^6 with the molecular size N. However, this unfavorable scaling is reduced by applying a Cholesky-decomposition of energy denominators as proposed by Hesselman.[67] The dRPA + SOSEX (we shall use SOSEX for short) correlation energy is obtained as

$$E_c^{SOSEX} = \frac{1}{2}\mathrm{tr}[\boldsymbol{KT}] \tag{3}$$

where $K_{ia,jb} = \langle ij\|ab\rangle$ are spin-singlet adapted antisymmetrized two electron repulsion integrals.

The RPAx (RPA or ring-CCD or rCCD) correlation energy is obtained according to eqs 10 and 13 in ref 65. We shall use RPA in this paper for RPAx.

We used Orca 3.0.1.for local pair natural orbital (LPNO)[68] coupled electron pair approximation (CEPA/1)[69] and domain-based DLPNO-CCSD(T)[70] calculations. The post-HF calculations were performed on AMD Opteron 6174 and Intel Xeon X5680 processors of the National Information Infrastructure Development Institute (NIIF).

For all calculations we use Dunning's correlation consistent aug-cc-pVXZ (AXZ) basis sets and the corresponding auxiliary density fitting basis sets (aug-cc-pVXZ/J, aug-cc-pVXZ/JK, and aug-cc-pVXZ/C). The extrapolated complete basis set (CBS) HF and MP2 correlation energies were calculated as shown in eqs 4 and 5

dx.doi.org/10.1021/ct5008263 | J. Chem. Theory Comput. XXXX, XXX, XXX−XXX

$$E_{CBS}^{HF} = E_{AQZ}^{HF} + \alpha(E_{AQZ}^{HF} - E_{ATZ}^{HF}) \quad (4)$$

and

$$E_{CBS}^{MP2c} = E_{AQZ}^{MP2c} + \beta(E_{AQZ}^{MP2c} - E_{ATZ}^{MP2c}) \quad (5)$$

where E_{CBS}^{HF} is the estimated HF/CBS, E_{AQZ}^{HF} is the HF/AQZ energy, etc. The extrapolation parameters are $\alpha = 0.269$ and $\beta = 0.712$. These parameters are slightly different from the earlier parameters optimized for the conformational energies of carbohydrates.[71]

The DLPNO-CCSD(T)/CBS energy is estimated according to eqs 6 and 7:

$$E_{CBS}^{MP2} = E_{CBS}^{HF} + E_{CBS}^{MP2c} \quad (6)$$

$$E_{CBS}^{CCSD(T)} = E_{CBS}^{MP2} + (E_{ATZ}^{CCSD(T)} - E_{ATZ}^{MP2}) \quad (7)$$

In this paper we use DLPNO-CCSD(T)/CBS electronic energies for reference.

The semilocal density functional methods cannot describe the purely nonlocal dispersion interaction. To account for the dispersion we applied the nonself-consistent VV10 nonlocal correction.[36] The electron density is only slightly altered by the VV10 correction, and thus the nonself-consistency results in a negligible error, as our analysis shows for these complexes. The VV10 correlation energy is given by the nonlocal term minus its local limit value ensuring the correction to vanish for the homogeneous electron gas (eq 8).

$$E_C^{VV10}[n(\vec{r})] = \frac{1}{2}\int\int n(\vec{r})\Phi(\vec{r},\vec{r}')n(\vec{r}')d^3\vec{r}d^3\vec{r}' - \int \varepsilon_C^{nl,unif}[n(\vec{r})]n(\vec{r})d^3\vec{r} \quad (8)$$

According to the local polarizability model, the nonlocal term can be written in a general form of the average interaction between two differential electron gas volumes, where the quality of the interaction is determined by a correlation kernel (eq 9)

$$\Phi(\vec{r},\vec{r}') = -\frac{3}{2}\frac{1}{g(\vec{r})g(\vec{r}')(g(\vec{r}) + g(\vec{r}'))} \quad (9)$$

where $g(\vec{r}) = \omega_0(\vec{r})R^2 + \kappa(\vec{r})$ with $R = |\vec{r} - \vec{r}'|$ distance and $\omega_0(\vec{r}) = (\omega_1^2(\vec{r}) + \omega_G^2(\vec{r}))^{1/2}$ local frequency, where $\omega_1(\vec{r}) = 3^{-1/2}\omega_p(\vec{r})$ is the local dipole resonance frequency computed from the local plasma frequency: $\omega_p(\vec{r}) = (4\pi n(\vec{r}))^{1/2}$. $\omega_G(\vec{r})$ is the local band gap, which might be approximated as shown in eq 10

$$\omega_G(\vec{r}) = \sqrt{C}\left|\frac{\nabla n(\vec{r})}{n(\vec{r})}\right|^2 \quad (10)$$

where $C = 0.0093$.

The second or $\kappa(\vec{r})$ term of $g(\vec{r})$ can be expressed as follows

$$\kappa(\vec{r}) = B\frac{v_F^2(\vec{r})}{\omega_P(\vec{r})} = 3B\frac{\omega_P(\vec{r})}{k_S^2(\vec{r})} \quad (11)$$

where $v_F(\vec{r}) = (3\pi^2 n(\vec{r}))^{1/3}$ is the local Fermi velocity, and k_S is the Thomas-Fermi screening wave vector. The correction can be fit to any density functional method by choosing an appropriate value for parameter B in eq 8. For revPBE, TPSS, rPW86PBE, PBE, and B2PLYP we used $B = 3.7$, 5.0, 5.9, 6.2, and 8.3, respectively.[72,73]

For double hybrid functionals we applied D2[74] and D3(BJ)[29] molecular mechanics dispersion corrections proposed by Grimme et al. The D2 correction contains a C_6 term (eq 12) and Tang-Toennies damping (eq 13)

$$E_{disp}^{D2} = -\frac{1}{2}\sum_{i\neq j} s_6 f_6(R_{ij})\frac{C_6^{ij}}{R_{ij}^6} \quad (12)$$

$$f_6(R_{ij}) = \frac{1}{1 + e^{-d(\frac{R_{ij}}{s_{r,6}\cdot R_0^{ij}} - 1)}} \quad (13)$$

where the global scaling factor of the energy is $s_6 = 0.4$ for mPW2PLYP, R_0^{ij} is the sum of the atomic van der Waals radii, the scaling factor of the distance is $s_{r,6} = 1.10$, and the parameter in the Tang-Toennies damping is $d = 20$. The D3(BJ) correction contains C_6 and C_8 terms (eq 14) and Becke-Johnson damping (eq 15)

$$E_{disp}^{D3(BJ)} = -\frac{1}{2}\sum_{i\neq j}\sum_{n=6,8} s_n\frac{C_n^{ij}}{R_{ij}^n + f^n(R_0^{ij})} \quad (14)$$

$$f(R_0^{ij}) = a_1 R_0^{ij} + a_2 \quad (15)$$

where $R_0^{ij} = (C_8^{ij}/C_6^{ij})^{1/2}$, the global scaling factors of the energy terms are $\{s_6, s_8\} = \{0.64, 0.9147\}$ for B2PLYP and $\{s_6, s_8\} = \{0.82, 0.29\}$ for PWPB95, while the parameters in the Becke-Johnson damping are $\{a_1, a_2\} = \{0.3065, 5.057\}$ for B2PLYP and $\{a_1, a_2\} = \{0, 7.3141\}$ for PWPB95.

For statistical analysis we calculated the mean deviation (MD), the mean absolute deviation (MAD), the minimum and maximum deviations from the reference, and the corrected sample standard deviation (CSSD or s) from the mean. In the computational chemistry literature, the MAD and the root-mean-square deviation are frequently used for method ranking. However, these are not measures for the precision of a method and consequently they might hide problems with precision. It is possible that a systematic error (e.g., systematic underbinding) is corrected with a random factor that shifts all energies toward overbinding. The MD and MAD might show considerable improvement, while the precision of the method is deteriorated. This is why we suggest CSSD to estimate the unbiased sample variance.

We used Gaussian 09 Revision C.01[75] to calculate the electrostatic potential maps and the static dipole polarizability tensors. We carried out basic-level density-fitted symmetry-adapted perturbation theory DF-SAPT0/jun-cc-pVDZ calculations (a modified aug-cc-pVDZ basis, with the diffuse functions on hydrogen and the diffuse d functions on heavy atoms removed)[76−78] for an energy decomposition analysis. SAPT analyses for several anion−π (HFB and TAZ) and cation−π−anion interaction energies were published in refs 12 and 9, respectively.

RESULTS AND DISCUSSION

First we discuss the 20 anion−π interaction energies between fluoride, chloride, bromide, nitrate, or carbonate ions and HFB, TFB, TFZ, or TAZ. The anions are bound along the symmetry axis of the aromatic ring as shown in Figure 1. The fully optimized RI-MP2(frozen core)/6-31++G(d,p) coordinates were taken from ref 1. Good agreement between RI-MP2 and MP2 equilibrium distances was observed as mentioned above. The frozen core and full MP2 calculations agree well except for the Br^- complexes, where the MP2(full) optimum is shorter by around 0.1 Å.[1,79] Notice that MP2(full) calculations with standard valence basis sets lead to controversial results,

dx.doi.org/10.1021/ct5008263 | J. Chem. Theory Comput. XXXX, XXX, XXX−XXX

and the application of the core−valence basis sets (e.g., cc-pCVTZ) is advised.[79] The equilibrium distances of the center of the anions from the plane of the π system in increasing order are the following: fluoride < carbonate < nitrate < chloride < bromide and TFZ < HFB < TAZ < TFB. The shortest distance is 2.385 Å for TFZ···F^-, and the longest distance is 3.487 Å for TFB···Br^- as shown in Table S1. The distances related to carbonate, nitrate, chloride, and bromide complexes are 6%, 15%, 24%, and 30% longer on average than those of the fluoride complexes, respectively. The distances related to HFB, TAZ, and TFB complexes are 6%, 8%, and 12% longer on average than those of the TFZ complexes, respectively.

The electrostatic potential (ESP) maps of HFB, TFB, TFZ, and TAZ are shown in Figure 3. Notice the relatively large positive charge on the TFZ surface that explains partly the relatively short distances for the TFZ complexes mentioned above. Qualitatively similar ESP maps can be found for HFB in Figure 1 of ref 80 and for TFB and TAZ in Figure 3 of ref 10. The quite uneven charge distribution of TAZ is well visible in Figure 3. The central area of the TFZ surface has a higher positive potential than of the TAZ surface due to the attached three fluorine atoms. However, in both rings, there is a large area of positive charge concentrated above the center of the molecules, which makes the molecules good candidates for establishing anion−π interactions. Inspection of the ESP maps of TFB, TFZ, and TAZ in Figure 3 show that displaced anion positions are advantageous (cf. large positive charges over several ring carbon atoms), thus displaced anions in the crystal structures might be expected.[18] These maps are helpful for visualization of the charge distribution in a monomer, but the electrostatic interaction of two monomers cannot be estimated from monomer ESPs reliably as other factors as discussed below also play an important role.

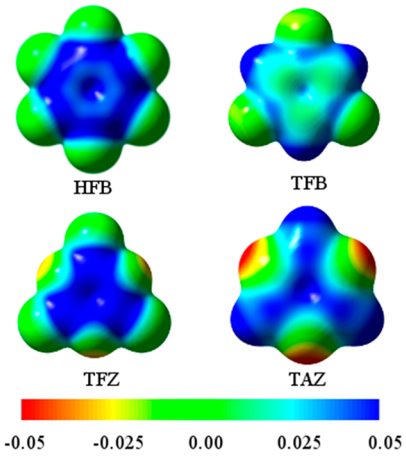

Figure 3. Electrostatic potential surfaces of hexafluorobenzene (HFB), 1,3,5-trifluorobenzene (TFB), 2,4,6-trifluoro-1,3,5-triazine (TFZ), and 1,3,5-triazine (TAZ) calculated at a PBE/ATZ electron isodensity value of 0.005 au. Electrostatic potential surface energies range from −0.05 (red) to +0.05 (blue) au.

To understand better the origin of the components of the interactions we analyze the Q_{zz} permanent quadrupole moment and the α_{zz} static polarizability components parallel to the main symmetry axis of the aromatic rings (cf. Figure 1). In benzene the Q_{zz} component of the quadrupole moment is negative ($Q_{zz}(C_6H_6)$ = −8.7 ± 0.5 B[81]), thus the anion-benzene electrostatic quadrupole interaction is repulsive. In HFB the six fluorine atoms change the polarity of the quadrupole to Q_{zz}(HFB) = +9.5 ± 0.5 B as shown in Figure 2 of ref 2. In TFB the missing three fluorine atoms lead to a much smaller, Q_{zz}(TFB) = +0.9 ± 0.1 B,[82] component, and the partial positive charge is located on the ipso carbon atoms (cf. Figure 3). In TAZ the quadrupole moment is very small again, Q_{zz}(TAZ) = +0.9 B, and somewhat larger alternating partial charges occur as shown in Figure 3. In TFZ the added three fluorine atoms make the ring atoms more positively charged leading to Q_{zz}(TFZ) = +8.2 B.

The ratios of the calculated α_{zz} static polarizability components of the HFB, TFB, TFZ, and TAZ are 90%, 93%, 70%, and 72% compared to α_{zz} for benzene (α_{zz} of benzene is around 6.7 $Å^3$ calculated with HF or MP2 methods). The four aromatic rings can be characterized as shown in Scheme 1. Notice that, while Q_{zz} shows a quite additive behavior depending on the number of the fluorine atoms, this additivity does not hold for α_{zz}.

Scheme 1. Classification of the Four Aromatic Compounds with Respect to the Magnitude of Q_{zz} and α_{zz}

		Q_{zz}	
		small	large
α_{zz}	small	TAZ	TFZ
	large	TFB	HFB

In order to analyze the magnitude of the anion−π interaction energy components, we have performed a density-fitted symmetry-adapted perturbation theory (SAPT) analysis.[83] Figure 4 shows the calculated SAPT0/jun-cc-pVDZ components of the interaction energies for the 20 complexes listed in Table 1. The repulsive exchange terms in Figure 4 are very large, see also ref 12, and variable (on average 131% of the total interaction energy and spanning the 74−200% range). The origin of the large exchange repulsion is the close orbital overlap.[12] Thus, conclusions of the earlier analyses[2] that neglect

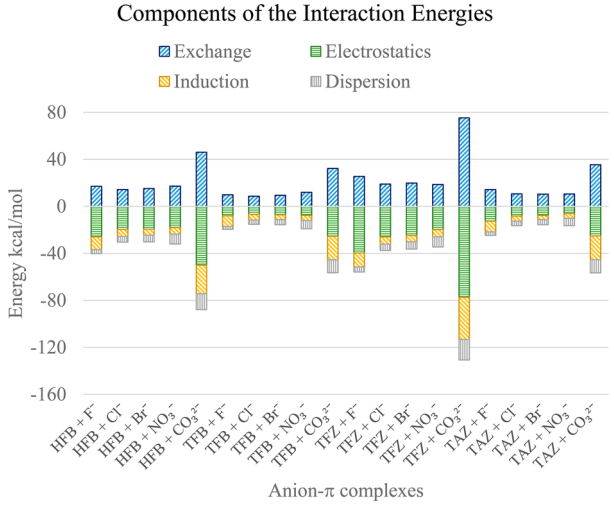

Figure 4. Symmetry-adapted perturbation theory SAPT0/jun-cc-pVDZ analysis of the electrostatic, exchange, induction, and dispersion components of the interaction energy of the anion−π binary complexes 1−20 in Figure 1 and Table 1.

dx.doi.org/10.1021/ct5008263 | J. Chem. Theory Comput. XXXX, XXX, XXX−XXX

Table 1. Benchmark Quality DLPNO-CCSD(T)/CBS Binding Interaction Energies, (kcal mol^{-1}), $E_{CBS}^{CCSD(T)}$, and MP2, HF, SOSEX, RPA, dRPA, and CEPA/1 Deviations from Benchmark Energies ($E - E_{CBS}^{CCSD(T)}$) of 20 Anion−π Complexes[l]

	complex[a]	$E_{CBS}^{CCSD(T)}$[b]	ΔE_{CP}^{MP2}[c]	ΔE_{CBS}^{HF}[d]	ΔE_{CBS}^{MP2}[e]	ΔE_{ATZ}^{SOSEX}	ΔE_{ATZ}^{RPA}	ΔE_{ATZ}^{dRPA}	$\Delta E_{ATZ}^{CEPA/1}$[f]
1	HFB + F^-	−21.08	2.77	2.59	0.32	−0.20	−0.63	−0.47	−0.20
2	HFB + Cl^-	−14.88	2.00	4.54	−1.31	0.38	−0.54	−0.14	−0.17
3	HFB + Br^-	−13.81	1.70	5.46	−1.20	0.79	−0.19	0.20	0.08
4	HFB + NO_3^-	−14.89	2.24	8.94	−1.37	0.76	−0.90	−0.43	−0.77
5	HFB + CO_3^{2-}	−38.36	5.29	10.87	−1.77	0.33	−1.88	−0.95	−0.42
6	TFB + F^-	−10.86	3.09	3.58	0.79	0.98	0.23	0.55	0.83
7	TFB + Cl^-	−7.43	2.64	4.69	−0.50	1.18	0.18	0.63	0.68
8	TFB + Br^-	−6.69	2.30	5.08	−0.72	1.19	0.16	0.59	0.04
9	TFB + NO_3^-	−8.66	3.04	8.50	−0.59	1.62	0.00	0.54	0.10
10	TFB + CO_3^{2-}	−24.31	6.98	10.66	−0.82	1.96	−0.66	0.71	0.45
11	TFZ + F^-	−27.67	3.44	2.68	0.33	−0.37	−0.51	−0.37	−0.38
12	TFZ + Cl^-	−18.03	3.14	5.71	−0.94	1.18	0.34	0.74	0.32
13	TFZ + Br^-	−15.87	1.87	6.32	−1.12	1.36	0.39	0.82	0.37
14	TFZ + NO_3^-	−16.07	3.06	8.76	−1.50	0.70	−0.75	−0.25	−0.60
15	TFZ + CO_3^{2-}	−51.07	14.13	13.07	−1.76	0.32	−0.95	−0.50	−0.27
16	TAZ + F^-	−11.90	2.20	4.37	−0.01	0.97	0.06	0.38	−0.16
17	TAZ + Cl^-	−7.26	2.04	5.42	−0.96	1.43	0.33	0.75	0.11
18	TAZ + Br^-	−6.37	1.36	5.57	−0.97	1.48	0.37	0.79	0.17
19	TAZ + NO_3^-	−7.32	1.98	7.54	−1.07	1.38	−0.06	0.41	−0.23
20	TAZ + CO_3^{2-}	−22.42	5.57	11.58	−1.63	2.10	−0.09	0.73	−0.47
	MD[g]		3.54	6.80	−0.84	0.98	−0.26	0.23	−0.03
	MAD[h]		3.54	6.80	0.98	1.03	0.46	0.55	0.34
	CSSD[i]		**2.87**	**3.04**	**0.72**	**0.65**	**0.59**	**0.55**	**0.42**
	Min[j]		1.36	2.59	−1.77	−0.37	−1.88	−0.95	−0.77
	Max[k]		14.13	13.07	0.79	2.10	0.39	0.82	0.83

[a]HFB = hexafluorobenzene, TFB = trifluorobenzene, TFZ = trifluorotriazine, TAZ = triazine. [b]Domain-based local pair natural orbital (DLPNO) method was applied for approximating the CCSD(T) energies at the aug-cc-pVTZ level, and focal point calculation was performed based on the MP2/CBS results. [c]The counterpoise correction (CP) is based on the 6-31++G(d,p) level (ref 1). [d]The complete basis set extrapolation (CBS) uses aug-cc-pVTZ and aug-cc-pVQZ results. [e]The sum of the complete basis set extrapolated MP2 correlation and HF energies. [f]Local pair natural orbital (LPNO) method was applied for approximating the CEPA/1 energies. [g]MD = mean deviation from benchmark. [h]MAD = mean absolute deviation from benchmark. [i]CSSD = corrected sample standard deviation from the mean. [j]Min = minimal deviation from the benchmark. [k]Max = maximal deviation from the benchmark. [l]The MP2 geometries used for these calculations were taken from ref 1.

the exchange repulsion based exclusively on inductive and electrostatic terms might be questionable.

The attractive electrostatic terms are also very large (on average 122% of the total interaction energy and spanning the 83−150% range) in agreement with the literature.[2,12] Figure 4 shows that the exchange and electrostatic terms are particularly large for 5 (HFB···CO_3^{2-}) and 15 (TFZ···CO_3^{2-}) complexes, as the centers of the CO_3^{2-} ions are quite close (at about 2.5 Å) to the aromatic ring center and the Q_{zz}s are large (cf. Scheme 1). For HFB and TFZ (large Q_{zz}s), the attractive electrostatic terms overcompensate the repulsive exchange terms, while for TFB and TAZ (small Q_{zz}s) the repulsive exchange terms overcompensate the attractive electrostatic terms as shown in Figure 4.

The induction energy components are smaller (on average 60% of the total interaction energy and spanning the 33−96% range; see also ref 12 for HFB and TAZ complexes). The induction is particularly important in the interactions of 6 (TFB···Cl^-, 94% of the total interaction energy) and 20 (TAZ···CO_3^{2-}, 96% of the total interaction energy). Notice that for TFB and TAZ the Q_{zz} components are small (cf. Scheme 1). Figure 4 shows that the induction energy components are particularly large for CO_3^{2-} containing complexes.

Several earlier studies have also suggested that dispersion forces, which are generally important in weak interactions involving aromatic rings, play only a minor role in anion−π bonding.[1,2] The dispersion energy component is particularly interesting as HF calculations miss this component completely, and the semilocal DFT calculations miss the long-range part of it. In the SAPT0 energy partition the dispersion component is the difference of the SAPT0 and the HF interaction energy (the HF interaction energy is composed of exchange, electrostatic and induction components). Larger polarizability might lead to stronger dispersion interaction (larger electron correlation energy), depending on the anion−π distance. We have calculated the MP2/ATZ polarizabilities of the free fluoride, chloride, bromide, nitrate, and carbonate ions that are 1.3, 4.1, 5.9, 5.1, and 8.2 Å^3, respectively. Notice that, except for fluoride, the polarizability values are comparable to the α_{zz} values (4.7−6.2 Å^3) of the aromatic rings discussed above. The dispersion energy components are smaller indeed but non-negligible in many complexes (on average 50% of the total interaction energy and spanning the 14−107% range, see also ref 12). The dispersion energy component of the interaction is the least important for fluoride complexes (due to the small polarizability of fluoride ions) and most important for bromide and nitrate complexes of TAZ and TFB characterized by small Q_{zz} (up to 70−107%). So in these complexes the binding arises completely or almost completely from the attractive dispersion interaction. Large dispersion attraction is observed for carbonate complexes (cf. large polarizability), but the relative importance of dispersion is smaller due to the large electrostatic components arising from the two negative charges.

dx.doi.org/10.1021/ct5008263 | J. Chem. Theory Comput. XXXX, XXX, XXX−XXX

Table 1 reports 20 new benchmark DLPNO-CCSD(T)/CBS binding interaction energies. Our CCSD(T) benchmark energies show reasonable agreement with nine HFB, TFB, and TFZ halide ion complex binding energies published in ref 84, but we used CCSD(T)/ATZ energies for CBS energy estimation, as shown by eq 7, instead of the less accurate and precise CCSD(T)/ADZ energies published in ref 84. Results in ref 85 show that the ATZ basis set is suitable to obtain reasonable results combined with the RI-MP2 method for various benzene and pyrazine anion− and cation−π complexes.

In Table 1 we also show the energy deviations, $\Delta E_{CP}^{MP2} = (E_{CP}^{MP2} - E_{CBS}^{CCSD(T)})$, where E_{CP}^{MP2} is a basis set superposition error (BSSE) corrected counterpoise (CP) MP2/6-31++G(d,p) energy taken from ref 1. Earlier these energies were used as benchmark binding energies; however, inspection of the large deviations, up to 14 kcal mol^{-1}, between DLPNO-CCSD(T)/CBS and CP-MP2 binding energies shown in Table 1 yields that these benchmark energies are inaccurate and imprecise, thus an earlier conclusion[1] about the good performance of MPWB1K functional[86] is questionable. The BSSE correction to binding energies of MP2/6-31++G(d,p), MP2/6-311++G(d,p), MP2/ADZ, and MP2/ATZ model chemistries is analyzed in ref 79, and the energies were compared to MP2/CBS(D,T) binding energies for TAZ···F$^-$, Cl$^-$, and Br$^-$ complexes. In this work we have calculated the considerably more accurate MP2/CBS(T,Q) energies according to eq 5 as shown in Table 1. This makes possible to re-evaluate the results of ref 79. For TAZ···F$^-$ the binding energy converges quickly with the basis set, the MP2/ADZ binding energy in ref 79 has a small basis set error around 0.3 kcal mol^{-1}, and the MP2/AQZ binding energy in Table S2 has a negligible basis set error of 0.15 kcal mol^{-1}. Applying the CP correction worsens these good and almost converged results by almost 2 kcal mol^{-1} for the ADZ basis set rendering this BSSE correction useless for this complex. Applying CP to MP2/6-31++G(d,p) binding energy that has 0.6 kcal mol^{-1} error results in inaccurate energies with errors more than 2.4 kcal mol^{-1}. For TAZ···Cl$^-$ the binding energy is sensitive to the basis set, and it is an example where MP2/CBS(D,T) extrapolation fails compared to MP2/CBS(T,Q) extrapolation. Due to the unreliable DZ basis set error here the D,T extrapolation goes in the opposite way (−8.4, −8.56, and −8.62 kcal mol^{-1}, D, T, and CBS binding energies in ref 79) than the T,Q extrapolation (−8.49, −8.33, and −8.22 kcal mol^{-1}, T, Q, and CBS binding energies in Table S2), thus the MP2/CBS(D,T) energy in ref 79 has 0.4 kcal mol^{-1} error. For this complex the CP correction to ADZ and ATZ basis sets is smaller, and the BSSE corrected CP-MP2/ATZ result in ref 79 has only 0.4 kcal mol^{-1} deviation. Interestingly MP2/6-31++G(d,p) and MP2/6-311++G(d,p) binding energies have relatively small overbinding errors (0.6 and 1.3 kcal mol^{-1}, respectively), but the 3.6 and 4 kcal mol^{-1} CP corrections yield around 2−3 kcal mol^{-1} underbinding error making these energies unsuitable for benchmark. For TAZ···Br$^-$ the comparison is more difficult as a slightly different equilibrium distance is used in refs 79 and 1, but for this complex again the CBS(D,Z)[79] and CBS(T,Q) extrapolation (cf. Table S2) goes in the opposite way. For this complex again the BSSE corrected MP2/6-31++G(d,p), MP2/6-311++G(d,p), and MP2/ATZ binding energies show around 2 kcal mol^{-1} errors. These inaccurate and imprecise BSSE overcompensations are the origins of the large and random ΔE_{CP}^{MP2} underbinding deviations in Table 1.

The HF/CBS deviations, $\Delta E_{CBS}^{HF} = (E_{CBS}^{HF} - E_{CBS}^{CCSD(T)})$, in Table 1, show the importance of the missing correlation energy and the vdW interaction as discussed above. The absolute value of the correlation energy is smaller for the halogen anion complexes (2.6−5.5 kcal mol^{-1}), and it is considerably larger for NO_3^- (8−9 kcal mol^{-1}) and CO_3^{2-} complexes (11−13 kcal mol^{-1}). Despite the short interaction distance in the fluoride complexes (cf. 2.39−2.75 Å given in ref 1), the correlation energy is only a small fraction of the total interaction energy (cf. around 2.6 kcal mol^{-1}, 10−12% errors of the HF/CBS interaction energies for HFB and TFZ···F$^-$ complexes in Table 1). These results agree with the SAPT0 results in Figure 4, and they can be explained by the small polarizability of the fluoride ion.

In agreement with the SAPT0 analysis results for TFB···Br$^-$, NO_3^-, TAZ···Cl$^-$, Br$^-$, and NO_3^- complexes, the origin of the binding energy can be attributed in 75−100% to electron correlation (dispersion) effects. This can be explained by the small quadrupole moments for TFB and TAZ and the large polarizabilities of Cl$^-$, Br$^-$, and NO_3^- discussed above. This fact contradicts an earlier supposition in the literature that the dispersion is not important for anion−π interactions. For HFB and TFZ···NO_3^- complexes, the correlation energy is about 55−60% of the total interaction energy, in perfect agreement with the SAPT0 dispersion energy component. The two negative charges of the carbonate ion makes the electrostatic interaction much larger than the dispersion interaction. Notice the particularly stable complexes of HFB and TFZ···CO_3^{2-} (at about 2.5 Å equilibrium distances) where the large positive Q_{zz} interacts with the two negative charges result in −38.36 and −51.07 kcal mol^{-1} interaction energies, respectively (cf. Table 1 and see also Figure 4 for SAPT0 analysis). The correlation energy vdW contributions to the interaction energies are also large, −10.87 and −13.07 kcal mol^{-1}, respectively (cf. Table 1).

Statistical analysis of the deviations in Table 1 shows that LPNO-CEPA/1/ATZ interaction energies agree best with the DLPNO-CCSD(T)/CBS energies. RPA and dRPA/ATZ perform almost equally well, and they provide only slightly worse agreement with the benchmark energies than the LPNO-CEPA/1. The SOSEX performs slightly worse than the dRPA. The statistical analysis shows that the MP2/ATZ (cf. MAD = 1.64 kcal mol^{-1} and CSSD = 1.17 kcal mol^{-1} in Table S2) or the more expensive MP2/AQZ (cf. MAD = 1.22 kcal mol^{-1} and CSSD = 0.85 kcal mol^{-1} in Table S2) perform worse than the dRPA/ATZ (cf. MAD = 0.53 kcal mol^{-1} and CSSD = 0.55 kcal mol^{-1} in Table 1). Even after the CBS extrapolation the MP2 results remain worse (cf. MAD = 0.98 kcal mol^{-1} and CSSD = 0.72 kcal mol^{-1} in Table 1) than the dRPA/ATZ results. The five correlation energy calculation methods analyzed here can be classified according to the increasing deviations (MD, MAD, and CSSD) from the reference as follows: LPNO-CEPA/1 < RPA ≈ dRPA < SOSEX < MP2 (cf. Table 1 and Table S1 results with the ATZ basis set).

We have performed a CPU-time based efficiency analysis of the above-mentioned correlation energy calculations, but notice that such analysis is always limited by the uncertainties arising from the actual computational environment (hardware, operating system, compiler optimizations, run time environment, etc.). We have selected 3 complexes from Table 1: the smallest, complex 16, TAZ···F$^-$, a medium sized, complex 1, HFB···F$^-$, and one of the largest, complex 5, HFB···CO_3^{2-}. These complexes require 391, 598, and 736 Gaussian ATZ basis functions for calculations and contain 38, 66, and 90

dx.doi.org/10.1021/ct5008263 | J. Chem. Theory Comput. XXXX, XXX, XXX−XXX

Table 2. VV10 Corrected rPWPBE, TPSS, revPBE, PBE, B2PLYP, D3(BJ) Corrected PWPB95, B2PLYP, and D2 Corrected mPW2PLYP Deviations from Benchmark ($E - E_{CBS}^{CCSD(T)}$) of 20 Anion−π Complexes (kcal mol^{-1})[g]

	complex[a]	$\Delta E_{ATZ}^{rPWPBE-VV}$	$\Delta E_{ATZ}^{TPSS-VV}$	$\Delta E_{ATZ}^{revPBE-VV}$	ΔE_{ATZ}^{PBE-VV}	$\Delta E_{ATZ}^{B2PLYP-VV}$	$\Delta E_{ATZ}^{PWPB95-D3}$	$\Delta E_{ATZ}^{B2PLYP-D3}$	$\Delta E_{ATZ}^{mPW2PLYP-D2}$
1	HFB + F^-	0.41	0.81	2.09	1.24	0.03	0.36	0.83	−0.32
2	HFB + Cl^-	−0.22	0.19	0.72	0.42	−0.47	−0.32	−0.15	−0.38
3	HFB + Br^-	1.23	1.58	1.98	1.79	−0.81	−0.57	−0.63	−0.79
4	HFB + NO_3^-	0.46	0.87	1.29	1.09	−1.07	0.24	−0.22	−0.91
5	HFB + CO_3^{2-}	−2.66	−3.01	−1.62	−1.90	−2.75	−1.15	−1.44	−2.35
6	TFB + F^-	−0.17	0.45	1.07	0.50	0.38	0.64	1.01	0.21
7	TFB + Cl^-	−0.06	0.49	0.67	0.49	0.12	0.47	0.34	0.31
8	TFB + Br^-	1.20	1.67	1.80	1.71	−0.40	0.05	−0.32	−0.27
9	TFB + NO_3^-	0.44	1.12	1.13	1.00	−0.20	1.04	0.40	0.00
10	TFB + CO_3^{2-}	−9.74	−3.18	−2.82	−2.78	−1.65	−0.64	−0.68	−1.28
11	TFZ + F^-	0.02	−0.07	1.54	0.55	−0.20	0.15	0.78	−0.33
12	TFZ + Cl^-	0.52	0.71	1.35	0.98	0.08	0.58	0.47	0.20
13	TFZ + Br^-	1.65	1.65	2.23	1.99	−0.64	−0.07	−0.40	−0.60
14	TFZ + NO_3^-	−0.05	0.14	0.68	0.36	−1.18	0.03	−0.22	−1.05
15	TFZ + CO_3^{2-}	−4.16	−6.93	−4.44	−4.89	−3.72	−2.83	−2.01	−2.67
16	TAZ + F^-	−1.55	−0.98	−0.42	−1.11	−0.31	0.08	0.39	−0.41
17	TAZ + Cl^-	−0.73	−0.20	−0.11	−0.36	−0.15	0.08	0.05	0.04
18	TAZ + Br^-	0.46	0.91	0.96	0.79	−0.60	−0.31	−0.54	−0.47
19	TAZ + NO_3^-	−0.88	−0.18	−0.31	−0.53	−0.77	0.31	−0.26	−0.61
20	TAZ + CO_3^{2-}	−12.62	−7.69	−7.38	−7.61	−3.18	−2.16	−2.28	−2.51
	MD[b]	−1.32	−0.58	0.02	−0.31	−0.87	−0.20	−0.24	−0.71
	MAD[c]	1.96	1.64	1.73	1.60	0.93	0.58	0.67	0.78
	CSSD[d]	**3.66**	**2.65**	**2.43**	**2.40**	**1.13**	**0.93**	**0.88**	**0.88**
	Min[e]	−12.62	−7.69	−7.38	−7.61	−3.72	−2.83	−2.28	−2.67
	Max[f]	1.65	1.67	2.23	1.99	0.93	1.04	1.01	0.78

[a]HFB = hexafluorobenzene, TFB = trifluorobenzene, TFZ = trifluorotriazine, TAZ = triazine. [b]MD = mean deviation from benchmark. [c]MAD = mean absolute deviation from benchmark. [d]CSSD = corrected sample standard deviation from the mean. [e]Min = minimal deviation from the benchmark. [f]Max = maximal deviation from the benchmark. [g]The MP2 geometries used for these calculations were taken from ref 1.

valence electrons, respectively. All time comparisons are related to the ATZ basis set and to the CPU times required for various correlation energy calculations (the CPU times of the HF calculations are excluded from the following comparisons). We select the CPU times of dRPA correlation energy calculations as reference. These are 2, 17, and 46 min, respectively. For the largest complex SOSEX calculation requires about 11% more CPU time than the dRPA calculation. The LPNO-CEPA/1 correlation energy calculation requires 17, 5.5, and 6.2 times more CPU time than the dRPA correlation energy calculation for the smallest, medium, and the largest complexes, respectively. This shows that the LPNO-CEPA/1 scales considerably better than the dRPA, the latter scales close to the fourth power (the dRPA formal scaling is fourth power), while the former scales around the third power for the complexes studied here. The DLPNO-CCSD(T) correlation energy calculation is about 33 times more expensive than that of dRPA correlation energy calculation and scales slightly worse. The RPA correlation energy calculation is the most expensive, the CPU times compared to the dRPA increase by around 130, 330, and 550 times for the smallest, medium, and the largest complexes, respectively. The MP2 correlation energy calculation is the fastest by far (0.7, 4, and 9 min, respectively) and it scales better than the dRPA (although the formal scaling of MP2 is the fifth power). The correlation energy calculation methods can be classified according to the increasing CPU times as follows: MP2 ≪ dRPA ≈ SOSEX < LPNO-CEPA/1 ≪ DLPNO-CCSD(T) < RPA (all with the ATZ basis set). The correlation energy calculation methods can be classified according to the scaling with the system size as follows: LPNO-CEPA/1 < MP2 < dRPA ≈ SOSEX < DLPNO-CCSD(T) < RPA.

We can conclude that the dRPA/ATZ is quite accurate, precise, and efficient, and it can be suggested for benchmarking anion−π interactions on moderately large systems. LPNO-CEPA/1 scales better than the dRPA, so for very large systems the former method can be more accurate, precise, and efficient.

In order to study basis set dependence, we calculated the dRPA energies of 65 hydrocarbons from CH_4 to C_6H_6 with AXZ basis sets with increasing cardinal numbers: X = {T, Q, 5, 6}. The optimized B3LYP/6-31G(2df,p) geometries were taken from Computational Chemistry Comparison and Benchmark Database.[87] The dRPA correlation energy converges to the basis set limit as follows

$$E_{AXZ}^{dRPAc} = E_{CBS}^{dRPAc} + AX^{-n} \quad (16)$$

where the statistical average n = 2.566. We suggest a two-point CBS(T, Q) extrapolation scheme, as we did for the MP2c in eq 5 but with larger β = 0.916. (A larger value of β shows that dRPAc converges to the basis set limit slower than MP2c.) With this parameter we obtained MD = 0.016 kcal mol^{-1} and CSSD = 0.16 kcal mol^{-1} compared to our most precise four point {T, Q, 5, 6} fitted extrapolated values. For 63 hydrocarbons the value of β is in the range of 0.89−0.94. This relatively small uncertainty in the extrapolation might lead to small error in the extrapolated correlation energy as shown above.

Using our new extrapolation scheme, we determined dRPA/CBS interaction energies for four TAZ anion complexes from dRPA/ATZ and AQZ interaction energies (Table S3). The

dx.doi.org/10.1021/ct5008263 | J. Chem. Theory Comput. XXXX, XXX, XXX−XXX

Table 3. Benchmark dRPA Interaction Energies and VV10 Corrected TPSS, revPBE, PBE, D3(BJ) Corrected B2PLYP and D2 Corrected mPW2PLYP Deviations from the Benchmark ($E - E_{ATZ}^{dRPA}$) of 30 π−Anion−π' Complexes (kcal mol^{-1})[g]

	complex[a]	E_{ATZ}^{dRPA}	$\Delta E_{ATZ}^{TPSS-VV}$	$\Delta E_{ATZ}^{revPBE-VV}$	ΔE_{ATZ}^{PBE-VV}	$\Delta E_{ATZ}^{B2PLYP-D3}$	$\Delta E_{ATZ}^{mPW2PLYP-D2}$
21	HFB + F^- + TFB	−30.72	1.62	3.57	2.24	1.58	−0.16
22	HFB + Cl^- + TFB	−21.47	0.46	1.14	0.72	−0.27	−0.44
23	HFB + Br^- + TFB	−19.30	2.00	2.54	2.32	−1.83	−1.87
24	HFB + NO_3^- + TFB	−23.08	2.31	2.69	2.50	0.04	−0.94
25	HFB + CO_3^{2-} + TFB	−59.66	−1.62	0.04	−0.16	−0.32	−1.59
26	HFB + F^- + TFZ	−46.02	2.15	4.75	3.19	2.08	0.19
27	HFB + Cl^- + TFZ	−30.65	0.61	1.79	1.22	−0.31	−0.68
28	HFB + Br^- + TFZ	−27.34	2.17	3.05	2.72	−2.00	−2.28
29	HFB + NO_3^- + TFZ	−29.94	2.16	2.93	2.60	0.19	−1.15
30	HFB + CO_3^{2-} + TFZ	−79.81	−3.72	−0.68	−1.12	−0.47	−1.83
31	HFB + F^- + TAZ	−31.72	0.59	2.44	1.02	1.11	−0.59
32	HFB + Cl^- + TAZ	−21.15	−0.27	0.33	−0.15	−0.67	−0.83
33	HFB + Br^- + TAZ	−18.81	1.22	1.68	1.38	−2.14	−2.16
34	HFB + NO_3^- + TAZ	−21.73	1.25	1.48	1.18	−0.43	−1.36
35	HFB + CO_3^{2-} + TAZ	−57.09	−5.64	−4.19	−4.57	−1.88	−2.90
36	TFB + F^- + TFZ	−36.57	0.73	2.90	1.48	1.42	−0.25
37	TFB + Cl^- + TFZ	−23.43	0.05	0.82	0.33	−0.55	−0.77
38	TFB + Br^- + TFZ	−20.70	1.51	2.13	1.84	−2.00	−2.10
39	TFB + NO_3^- + TFZ	−23.77	1.28	1.76	1.45	−0.16	−1.27
40	TFB + CO_3^{2-} + TFZ	−68.20	−5.70	−3.40	−3.55	−1.46	−2.47
41	TFB + F^- + TAZ	−21.21	−0.88	0.29	−0.90	0.35	−1.04
42	TFB + Cl^- + TAZ	−13.23	−0.86	−0.61	−1.01	−0.93	−0.90
43	TFB + Br^- + TAZ	−11.65	0.64	0.70	0.47	−2.07	−1.90
44	TFB + NO_3^- + TAZ	−14.98	0.29	0.15	−0.13	−0.88	−1.54
45	TFB + CO_3^{2-} + TAZ	−42.98	−7.87	−9.68	−7.41	−2.92	−3.61
46	TFZ + F^- + TAZ	−37.49	−0.18	1.93	0.41	0.98	−0.67
47	TFZ + Cl^- + TAZ	−23.14	−0.65	0.03	−0.53	−0.92	−1.12
48	TFZ + Br^- + TAZ	−20.18	0.77	1.31	0.94	−2.32	−2.40
49	TFZ + NO_3^- + TAZ	−22.37	0.29	0.64	0.21	−0.65	−1.72
50	TFZ + CO_3^{2-} + TAZ	−65.38	−9.03	−6.76	−7.28	−2.78	−3.61
	MD[b]		−0.48	0.53	0.05	−0.67	−1.47
	MAD[c]		1.95	2.21	1.83	1.19	1.48
	CSSD[d]		**2.97**	**3.03**	**2.63**	**1.31**	**0.95**
	Min[e]		−9.03	−9.68	−7.41	−2.92	−3.61
	Max[f]		2.31	4.75	3.19	2.08	0.19

[a]HFB = hexafluorobenzene, TFB = trifluorobenzene, TFZ = trifluorotriazine, TAZ = triazine. [b]MD = mean deviation from benchmark. [c]MAD = mean absolute deviation from benchmark. [d]CSSD = corrected sample standard deviation from the mean. [e]Min = minimal deviation from the benchmark. [f]Max = maximal deviation from the benchmark. [g]The MP2 geometries used for these calculations were taken from ref 1.

results in Table S3 show about 0.6−1.3 kcal mol^{-1} shift in the underbinding direction. This is in agreement with the earlier observation that dRPA systematically underbinds the weakly interacting complexes. The good dRPA/ATZ results can be attributed to a slight overbinding error of the ATZ basis set that might efficiently compensate the underbinding error of the dRPA. As both dRPA and the AVTZ basis sets show quite systematic error and behave well, this might result in generally good results. However, the validity of this observation must be tested in further studies.

Next we used our new benchmark energies to rank various approximate density functionals. Notice that calculating anions with common semilocal and hybrid density functionals requires caution, as a fraction of the electron leaks to infinity when sufficiently large basis sets are employed.[88,89] The origin of this is the self-interaction error that leads to incorrect exponential decay of the exchange potential in the asymptotic region (instead of the exact $-1/r$). The effect of the self-interaction error is particularly large for anions and leads to positive HOMO energies.[90,91] Using a finite basis set stabilizes this unbound state artificially. In the presence of cations, fractional charge transfer occurs even with finite basis sets, due to n-electron self-interaction error.[92] Despite these errors, approximate density functional methods give useful anion energies and electron affinities.[93]

In Table 2 we show the VV10 dispersion corrected errors for PBE, TPSS, and revPBE. We also tested the original rPWPBE GGA functional suggested for VV10, but these results are the poorest as shown in Table 2. We show the uncorrected and dispersion corrected DFT binding energies and the magnitude of D3, D2, and VV10 correction in Tables S3−S7 of the Supporting Information. The accuracy of the VV10 corrected PBE and TPSS is comparable to the accuracy of the MP2, but the precision (CSSD) is much worse. For brevity we do not discuss here the similar results for standard hybrid functionals like B3LYP, PBE0, TPSSh, or ω-B97x-D; the interested readers should refer to refs 1, 49, and 84 and references cited therein. The double hybrid functionals perform reasonably well and very similarly to each other but do not reach the precision of the dRPA (cf. CSSD(dRPA) = 0.55 kcal mol^{-1} vs CSSD-

dx.doi.org/10.1021/ct5008263 | J. Chem. Theory Comput. XXXX, XXX, XXX−XXX

(PWPB95-D3) = 0.93 kcal mol^{-1} in Tables 1 and 2). The double hybrids are inaccurate without dispersion correction (they underbind by 1.65 or 0.88 kcal mol^{-1} on average), but they are quite precise as the CSSD is around 0.5 kcal mol^{-1} (cf. Table S2) comparable to the CSSD of the dRPA. D2 or D3(BJ) dispersion corrections efficiently correct systematic overbinding error, but these corrections make the methods considerably less precise (cf. CSSD is increased to 0.88 or 0.93 kcal mol^{-1} in Table 2). This shows the somewhat random nature of these *a posteriori* D2 and D3(BJ) corrections. The recent D3(BJ) parameter set performs well on many, somewhat restricted data sets, but the large parameter set combined with various functionals might make such methods less transparent. The performance for systems and oxidation states not included in the training set is uncertain as dispersion coefficients strongly depend upon ionization, and this does not work properly in a force field type dispersion correction. This might lead to a somewhat random nature of the D3(BJ) corrections as observed here.

Comparison of MADs and CSSDs in Tables 1 and 2 shows the following ranking from the best to worst: dRPA < PWPB95−D3(BJ) < B2PLYP−D3(BJ) < mPW2PLYP−D2 < B2PLYP−VV10 ≪ PBE−VV10 ≈ TPSS−VV10 < revPBE−VV10 ≪ rPWPBE−VV10. All calculations used the ATZ basis set.

Our new dRPA/ATZ binding energies used as a benchmark for 30 π−anion−π' sandwich complexes are shown in Table 3. All semilocal functionals need further improvements, as even the best PBE-VV10 methods show relatively large MAD = 1.83 and CSSD = 2.63 kcal mol^{-1} (cf. Table 3). Without VV10 vdW correction all semilocal functionals show serious underbinding error (8−15 kcal mol^{-1} as shown in Tables S8 and S9), as expected. The VV10 vdW energy corrections are shown in Table S10. The more expensive double hybrid functionals perform considerably better here. The most accurate is the B2PLYP-D2/ATZ, and the most precise is the mPW2PLYP-D2/ATZ model chemistry. Without dispersion correction these model chemistries show 2−3 kcal mol^{-1} underbinding error (cf. Tables S8 and S9). Comparison dRPA/ATZ binding energies with the earlier RI-MP2(FC)/6-31++G(d,p) results[1] show a serious disagreement up to almost 20 kcal mol^{-1}. Comparison of MADs and CSSDs in Table 3 shows the following ranking from the best to worst: B2PLYP−D3(BJ) < mPW2PLYP−D2 ≪ PBE−VV10 < TPSS−VV10 < revPBE−VV10. All calculations used the ATZ basis set. Notice that this ranking is consistent with the previous ranking, with the exception that here PBE−VV10 is clearly better than TPSS−VV10. The ranking of B2PLYP−D3(BJ) and mPW2PLYP−D2 is not evident, as B2PLYP−D3(BJ) is more accurate but considerably less precise than mPW2PLYP−D2. The transferability of the errors and observations from anion−π complexes to ternary π−anion−π' sandwich complexes suggests that some kind of additivity effects[1] exist within this class of molecules.

The additivity of the interaction can be analyzed in the π−anion−π' complexes using all possible combinations of the four aromatic compounds and the five anions presented in this paper. It was observed earlier that the equilibrium distances in the binary π−anion and the ternary π−anion−π' are very similar.[1] The largest variation can be found in complex TFB···Br$^-$···TAZ (43 in Table 3), where the TFB···Br$^-$ and the Br$^-$···TAZ distances are longer by 0.063 and 0.094 Å, respectively. The additivity is approximately valid for the interaction energies, as the interactions are only slightly affected by the presence of the second aromatic ring on the other side of the anions. For example the −11.65 kcal mol^{-1} dRPA/ATZ interaction energy of the TFB···Br$^-$···TAZ ternary complex (cf. 43 in Table 3) is reasonably approximated by the sum of the TFB···Br$^-$ and the Br$^-$···TAZ interaction energies, −6.11 and −5.59 kcal mol^{-1}, respectively. Notice that the interaction energies are quite insensitive to the distance, as the energy surface is very flat around the minima.

CONCLUSIONS

The correct description of the interaction between anions and aromatic rings might be used for the design of selective anion receptors and channels, and this is important for advances in the field of supramolecular chemistry. In this paper we focus on the so-called anion−π interaction. The anions are bound along the symmetry axis of the aromatic ring, as shown in Figure 1. The accurate, precise, and efficient calculation of this interaction is challenging, and inaccurate results are available in the literature. Here we propose benchmark quality solutions and detailed explanation of the origin of such interactions. The insight given in this paper might be used for future design and prediction of the properties of anion−π sandwiches and larger complexes.

We have calculated the α_{zz} static polarizability components parallel to the main symmetry axis of the aromatic rings (cf. Figure 1) for hexafluorobenzene (HFB), 1,3,5-trifluorobenzene (TFB), 2,4,6-trifluoro-1,3,5-triazine (TFZ), or 1,3,5-triazine (TAZ). These results and the experimental Q_{zz} permanent quadrupole moments show that the four molecules fall into four different classes with respect to the magnitude of Q_{zz} and α_{zz}: TAZ(small, small), HFB(large, large), TFZ(large, small), and TFB(small, large), respectively.

We have also calculated the electrostatic potential maps that show the uneven charge distribution on the surface of the aromatic rings and the electron withdrawing effects of the various fluorine substitutions. The off center positive charge distribution on the ESP maps of TFB, TFZ, and TAZ show that displaced anions might be stabilized. This explains the displaced anions observed in several crystal structures.

We have performed a symmetry-adapted perturbation theory analysis (SAPT0/jun-cc-pVDZ), DLPNO-CCSD(T)/CBS, MP2, HF, SOSEX, RPA, dRPA, LPNO-CEPA/1, VV10 corrected rPWPBE, TPSS, revPBE, PBE, B2PLYP, D3(BJ) corrected PWPB95, B2PLYP, and D2 corrected mPW2PLYP calculations for 20 fluoride, chloride, bromide, nitrate, or carbonate complexes of HFB, TFB, TFZ, or TAZ.

Our SAPT results show that the repulsive exchange and the attractive electrostatic, induction, and dispersion energy components are on average −131%, 122%, 60%, and 50% of the total interaction energy, respectively. The repulsive exchange, the attractive electrostatic, induction, and dispersion energy components vary from −74% to −200%, 83% to 150%, 33% to 96%, and 14% to 107% of the total interaction energy, respectively. The exchange and electrostatic terms are particularly large for HFB···CO_3^{2-} and TFZ···CO_3^{2-} complexes because the center of the CO_3^{2-} ion is relatively close to the aromatic ring center and HFB and TFZ Q_{zz}s are large. The induction is particularly important in the interactions of TFB···Cl$^-$ and TAZ···CO_3^{2-}, as the Q_{zz} components of TFB and TAZ are small. The vdW dispersion energy components are relatively small in the fluoride complexes, and they are particularly important for bromide and nitrate complexes of TFB and TAZ. Differences of DLPNO-CCSD(T)/CBS and

dx.doi.org/10.1021/ct5008263 | J. Chem. Theory Comput. XXXX, XXX, XXX−XXX

HF/CBS energies show good agreement with SAPT0 dispersion energy components.

Our results show that the investigated correlation energy calculation methods can be classified according to increasing deviations from the reference DLPNO-CCSD(T)/CBS interaction energies as LPNO-CEPA/1 < dRPA ≈ RPA < SOSEX < MP2. These density-fitted methods can be classified according to the increasing CPU times as MP2 ≪ dRPA ≈ SOSEX < LPNO-CEPA/1 ≪ DLPNO-CCSD(T) < RPA and according to the scaling with the system size as LPNO-CEPA/1 < MP2 < dRPA ≈ SOSEX < DLPNO-CCSD(T) < RPA, all with augmented triple-ζ (ATZ) basis set.

We can conclude that the dRPA/ATZ is quite accurate, precise, and efficient, and it can be suggested for benchmarking anion−π interactions on moderately large systems where DLPNO-CCSD(T) is too expensive. We show that the slight underbinding error of dRPA/CBS (0.6−1.3 kcal mol^{-1}) is efficiently compensated by the comparable overbinding error of the ATZ basis set. LPNO-CEPA/1 scales better than the dRPA, so for very large systems it can be more accurate, precise, and efficient. According to our results in agreement with ref 84, the counterpoise corrected (CP) MP2/6-31++G(d,p) energies suggested in ref 1 are not suitable for benchmarking.

We used our new benchmark energies to rank various approximate density functionals. Comparison of mean absolute deviations (MAD) and precisions (CSSD) shows the following ranking from the best to worst: PWPB95−D3(BJ) < B2PLYP−D3(BJ) < mPW2PLYP−D2 < B2PLYP−VV10 ≪ PBE−VV10 ≈ TPSS−VV10 < revPBE−VV10 ≪ rPWPBE−VV10. All calculations used the ATZ basis set. The double hybrid functionals with dispersion correction perform best, almost reaching the accuracy of the dRPA/ATZ binding energies but not the precision. Without dispersion correction all functionals underbind and show serious errors. We have also shown that the precision (CSSD) of the investigated D3(BJ) dispersion corrected double hybrid functionals deteriorates for the current set of complexes.

For 30 π−anion−π' sandwich complexes we have calculated dRPA/ATZ binding energies for benchmarks. For the investigated density functionals, we obtained the following ranking from the best to worst: B2PLYP−D3(BJ) < mPW2PLYP−D2 ≪ PBE−VV10 < TPSS−VV10 < revPBE−VV10. This ranking for π−anion−π' sandwich complexes is very similar to the previous ranking for anion−π complexes, and this suggests some kind of additivity effects.

Systematic comparison of our dRPA/ATZ energies shows that the ternary interaction energy can be calculated from the two corresponding binary interaction energies with negligible error. Consequently the energies are practically additive. The origin of this is the near equality of the equilibrium distances in the binary π−anion and the ternary π−anion−π' as observed earlier. Moreover the interaction energies are quite insensitive to the small variations of the π−anion−π' distances as the energy surface is sufficiently flat around the minima.

For future benchmarking of various efficient methods, we suggest using our new interaction energies. Among the investigated methods, the dRPA/ATZ model chemistry is quite accurate, precise, and efficient so we suggest using it for solving chemical and biological problems of similar size as those studied in this paper. If accuracy is more important than efficiency, then the more accurate LPNO-CEPA/1/ATZ is suggested, and because of the excellent scaling with size it might be more efficient for sufficiently large systems than dRPA. The most efficient but somewhat less precise methods are among the double hybrid functionals; for the present test set the PWPB95−D3(BJ) and B2PLYP−D3(BJ) are the best performers.

■ ASSOCIATED CONTENT

Supporting Information

Ten tables show the equilibrium distances and detailed energies for the 50 complexes discussed in this paper. This material is available free of charge via the Internet at http://pubs.acs.org.

■ AUTHOR INFORMATION

Corresponding Author

*E-mail: csonkagi@gmail.com.

Notes

The authors declare no competing financial interest.

■ ACKNOWLEDGMENTS

This work was supported by the Department of Energy under Grant No. DE-SC0010499. G.I.C. acknowledges the support by the New Hungary Development Plan (Project ID: TAMOP-4.2.1/B-09/1/KMR-2010-0002) at the BME project. The authors thank the Hungarian National higher education and research network for the computer time.

■ REFERENCES

(1) Garau, C.; Frontera, A.; Quiñonero, D.; Russo, N.; Deya, P. M. *J. Chem. Theory Comput.* **2011**, *7*, 3012−3018.

(2) Frontera, A.; Gamez, P.; Mascal, M.; Mooibroek, T. J.; Reedijk, J. *Angew. Chem., Int. Ed. Engl.* **2011**, *50*, 9564−9583.

(3) Lehn, J. M. *Supramolecular Chemistry. Concepts and Perspectives*; Wiley-VCH: Weinheim, 1995; p 31.

(4) Schneider, H. J. *Angew. Chem.* **2009**, *121*, 3982; *Angew. Chem., Int. Ed.* **2009**, *48*, 3924.

(5) Meyer, E. A.; Castellano, R. K.; Diederich, F. *Angew. Chem.* **2003**, *115*, 1244; *Angew. Chem., Int. Ed.* **2003**, *42*, 1210.

(6) Stivers, J. T.; Jiang, Y. L. *Chem. Rev.* **2003**, *103*, 2729.

(7) Ma, J. C.; Dougherty, D. A. *Chem. Rev.* **1997**, *97*, 1303.

(8) Crowley, P. B.; Golovin, A. *Proteins: Struct., Funct., Genet.* **2005**, *59*, 231.

(9) Kim, D.; Lee, E. C.; Kim, K. S.; Tarakeshwar, P. *J. Phys. Chem. A* **2007**, *111*, 7980−7986.

(10) Schottel, B. L.; Chifotides, H. T.; Dunbar, K. R. *Chem. Soc. Rev.* **2008**, *37*, 68−83.

(11) Estarellas, C.; Frontera, A.; Quiñonero, D.; Deyá, P. M. *Angew. Chem.* **2011**, *123*, 435; *Angew. Chem., Int. Ed.* **2011**, *50*, 415.

(12) Kim, D.; Tarakeshwar, P.; Kim, K. S. *J. Phys. Chem. A* **2004**, *108*, 1250−1258.

(13) Gamez, P.; Mooibroek, T. J.; Teat, S. J.; Reedijk, J. *Acc. Chem. Res.* **2007**, *40*, 435−444.

(14) http://www.ccdc.cam.ac.uk/Solutions/CSDSystem/Pages/CSD.aspx (accessed 20.10.2014).

(15) Dawson, R. E.; Hennig, A.; Weimann, D. P.; Emery, D.; Ravikumar, V.; Montenegro, J.; Takeuchi, T.; Gabutti, S.; Mayor, M.; Mareda, J.; Schalley, C. A.; Matile, S. *Nat. Chem.* **2010**, *2*, 533−538.

(16) Mareda, J.; Matile, S. *Chem.—Eur. J.* **2009**, *15*, 28−37.

(17) Perez-Velasco, A.; Gorteau, V.; Matile, S. *Angew. Chem.* **2008**, *120*, 935; *Angew. Chem., Int. Ed.* **2008**, *47*, 921.

(18) Kim, D. Y.; Singh, N. J.; Lee, J. W.; Kim, K. S. *J. Chem. Theory Comput.* **2008**, *4*, 1162−1169.

(19) Rolik, Z.; Kállay, M. *J. Chem. Phys.* **2011**, *134*, 124111.

(20) Hohenberg, P.; Kohn, W. *Phys. Rev.* **1964**, *136*, B864−B871.

(21) Kohn, W.; Sham, L. J. *Phys. Rev.* **1965**, *140*, A1133−38.

(22) Kohn, W.; Becke, A. D.; Parr, R. G. *J. Chem. Phys.* **1996**, *100*, 12974−12980.

(23) Cohen, A. J.; Mori-Sánchez, P.; Yang, W. *Science (80-.)* **2008**, *321*, 792−794.
(24) Becke, A. D. *J. Chem. Phys.* **2014**, *140*, 18A301.
(25) Wu, Q.; Yang, W. *J. Chem. Phys.* **2002**, *116*, 515−524.
(26) Goerigk, L.; Grimme, S. *J. Chem. Theory Comput.* **2011**, *7*, 291−309 and references therein.
(27) Tkatchenko, A.; Scheffler, M. *Phys. Rev. Lett.* **2009**, *102*, 073005.
(28) Grimme, S.; Antony, J.; Ehrlich, S.; Krieg, H. *J. Chem. Phys.* **2010**, *132*, 154104.
(29) Grimme, S.; Ehrlich, S.; Goerigk, L. *J. Comput. Chem.* **2011**, *32*, 1456−1465.
(30) Becke, A. D.; Johnson, E. R. *J. Chem. Phys.* **2005**, *123*, 154101.
(31) Görling, A.; Levy, M. *Phys. Rev. B* **1993**, *47*, 13105−13113.
(32) Görling, A.; Levy, M. *Phys. Rev. A* **1994**, *50*, 196−204.
(33) Dion, M.; Rydberg, H.; Schröder, E.; Langreth, D. C.; Lundqvist, B. I. *Phys. Rev. Lett.* **2004**, *92*, 22−25.
(34) Dion, M.; Rydberg, H.; Schröder, E.; Langreth, D.; Lundqvist, B. *Phys. Rev. Lett.* **2005**, *95*, 109902.
(35) Lee, K.; Murray, D.; Kong, L.; Lundqvist, B. I.; Langreth, D. C. *Phys. Rev. B* **2010**, *82*, 081101.
(36) Vydrov, O.; Voorhis, T. Van. *J. Chem. Phys.* **2010**, *133*, 244103.
(37) Langreth, D. C.; Perdew, J. P. *Solid State Commun.* **1975**, *17*, 1425−1429.
(38) Langreth, D. C.; Perdew, J. P. *Phys. Rev. B* **1977**, *15*, 2884.
(39) Langreth, D. C.; Perdew, J. P. *Phys. Rev. B* **1980**, *21*, 5469−5493.
(40) Axilrod, B. M.; Teller, E. *J. Chem. Phys.* **1943**, *11*, 299.
(41) Lu, D.; Nguyen, H.-V.; Galli, G. *J. Chem. Phys.* **2010**, *133*, 154110.
(42) Ruzsinszky, A.; Perdew, J. P.; Tao, J.; Csonka, G. I.; Pitarke, J. M. *Phys. Rev. Lett.* **2012**, *109*, 233203.
(43) Scuseria, G. E.; Henderson, T. M.; Sorensen, D. C. *J. Chem. Phys.* **2008**, *129*, 231101.
(44) Mori-Sánchez, P.; Cohen, A. J.; Yang, W. *Phys. Rev. Lett.* **2008**, *100*, 146401.
(45) Paier, J.; Janesko, B. G.; Henderson, T. M.; Scuseria, G. E.; Grüneis, A.; Kresse, G. *J. Chem. Phys.* **2010**, *132*, 094103.
(46) Paier, J.; Janesko, B. G.; Henderson, T. M.; Scuseria, G. E.; Grüneis, A.; Kresse, G. *J. Chem. Phys.* **2010**, *133*, 179902.
(47) Ruzsinszky, A.; Perdew, J. P.; Csonka, G. I. *J. Chem. Theory Comput.* **2010**, *6*, 127−134.
(48) Ruzsinszky, A.; Perdew, J. P.; Csonka, G. I. *J. Chem. Phys.* **2011**, *134*, 114110.
(49) Quiñonero, D.; Garau, C.; Frontera, A.; Ballester, P.; Costa, A.; Deyà, P. M. *J. Phys. Chem. A* **2005**, *109*, 4632−4637.
(50) Neese, F. *Wiley Interdiscip. Rev.: Comput. Mol. Sci.* **2012**, *2*, 73−78.
(51) Perdew, J. P.; Burke, K.; Ernzerhof, M. *Phys. Rev. Lett.* **1996**, *77*, 3865−3868.
(52) Perdew, J. P.; Burke, K.; Ernzerhof, M. *Phys. Rev. Lett.* **1998**, *80*, 890.
(53) Murray, E. D.; Lee, K.; Langreth, D. C. *J. Chem. Theory Comput.* **2009**, *5*, 2754−2762.
(54) Tao, J.; Perdew, J. P.; Staroverov, V. N.; Scuseria, G. E. *Phys. Rev. Lett.* **2003**, *91*, 146401.
(55) Grimme, S. *J. Chem. Phys.* **2006**, *124*, 034108.
(56) Becke, A. D. *Phys. Rev. B* **1988**, *38*, 3098−3100.
(57) Lee, C.; Yang, W.; Parr, R. G. *Phys. Rev. B* **1988**, *37*, 785−789.
(58) Schwabe, T.; Grimme, S. *Phys. Chem. Chem. Phys.* **2006**, *8*, 4398−4401.
(59) Adamo, C.; Barone, V. *J. Chem. Phys.* **1998**, *108*, 664−675.
(60) Goerigk, L.; Grimme, S. *J. Chem. Theory Comput.* **2011**, *7*, 291−309.
(61) Perdew, J. P. In *Proceedings of the 21st Annual International Symposium on the Electronic Structure of Solids*; Ziesche, P., Eschrig, H., Eds.; Akademie Verlag: Berlin, 1991; p 11.
(62) Becke, A. D. *J. Chem. Phys.* **1996**, *104*, 1040−1046.
(63) Whitten, J. L. *J. Chem. Phys.* **1973**, *58*, 4496.
(64) Rolik, Z.; Szegedy, L.; Ladjánszki, I.; Ladóczki, B.; Kállay, M. *J. Chem. Phys.* **2013**, *139*, 094105.
(65) Toulouse, J.; Zhu, W.; Savin, A.; Jansen, G.; Ángyán, J. G. *J. Chem. Phys.* **2011**, *135*, 084119.
(66) Sanderson, E. A. *Phys. Lett.* **1965**, *19*, 141−143.
(67) Heßelmann, A. *Phys. Rev. A* **2012**, *85*, 012517.
(68) Neese, F.; Hansen, A.; Liakos, D. G. *J. Chem. Phys.* **2009**, *131*, 064103.
(69) Neese, F.; Hansen, A.; Wennmohs, F.; Grimme, S. *Acc. Chem. Res.* **2009**, *42*, 641−648.
(70) Riplinger, C.; Neese, F. *J. Chem. Phys.* **2013**, *138*, 034106.
(71) Csonka, G. I.; Kaminsky, J. *J. Chem. Theory Comput.* **2011**, *7*, 988−997.
(72) Hujo, W.; Grimme, S. *J. Chem. Theory Comput.* **2011**, *7*, 3866−3871.
(73) Aragó, J.; Ortí, E.; Sancho-García, J. C. *J. Chem. Theory Comput.* **2013**, *9*, 3437−3443.
(74) Grimme, S. *J. Comput. Chem.* **2006**, *27*, 1787−1799.
(75) Frisch, M. J.; Trucks, G. W.; Schlegel, H. B.; Scuseria, G. E.; Robb, M. A.; Cheeseman, J. R.; Scalmani, G.; Barone, V.; Mennucci, B.; Petersson, G. A.; Nakatsuji, H.; Caricato, M.; Li, X.; Hratchian, H. P.; Izmaylov, A. F.; Bloino, J.; Zheng, G.; Sonnenberg, J. L.; Hada, M.; Ehara, M.; Toyota, K.; Fukuda, R.; Hasegawa, J.; Ishida, M.; Nakajima, T.; Honda, Y.; Kitao, O.; Nakai, H.; Vreven, T.; Montgomery, J. A., Jr.; Peralta, J. E.; Ogliaro, F.; Bearpark, M.; Heyd, J. J.; Brothers, E.; Kudin, K. N.; Staroverov, V. N.; Kobayashi, R.; Normand, J.; Raghavachari, K.; Rendell, A.; Burant, J. C.; Iyengar, S. S.; Tomasi, J.; Cossi, M.; Rega, N.; Millam, N. J.; Klene, M.; Knox, J. E.; Cross, J. B.; Bakken, V.; Adamo, C.; Jaramillo, J.; Gomperts, R.; Stratmann, R. E.; Yazyev, O.; Austin, A. J.; Cammi, R.; Pomelli, C.; Ochterski, J. W.; Martin, R. L.; Morokuma, K.; Zakrzewski, V. G.; Voth, G. A.; Salvador, P.; Dannenberg, J. J.; Dapprich, S.; Daniels, A. D.; Farkas, Ö.; Foresman, J. B.; Ortiz, J. V.; Cioslowski, J.; Fox, D. J. *Gaussian 09, Revision C.01*; Gaussian, Inc.: Wallingford, CT, 2009.
(76) Jeziorski, B.; Moszynski, R.; Szalewicz, K. *Chem. Rev.* **1994**, *94*, 1887−1930.
(77) Hohenstein, E. G.; Parrish, R. M.; Sherrill, C. D.; Turney, J. M.; Schaefer, H. F. *J. Chem. Phys.* **2011**, *135*, 174107.
(78) Hohenstein, E. G.; Sherrill, C. D. *J. Chem. Phys.* **2010**, *132*, 184111.
(79) Estarellas, C.; Lucas, X.; Frontera, A.; Quinonero, D.; Deyá, P. M. *Chem. Phys. Lett.* **2010**, *489*, 254−258.
(80) Ehrlich, S.; Moellmann, J.; Grimme, S. *Acc. Chem. Res.* **2013**, *46*, 916−926.
(81) Battaglia, M. R.; Buckingham, A. D.; Williams, J. H. *Chem. Phys. Lett.* **1981**, *78*, 421−423.
(82) Vrbancich, J.; Ritchie, G. L. D. *J. Chem. Soc., Faraday Trans. 2* **1980**, *76*, 648−659.
(83) Hohenstein, E. G.; Sherrill, C. D. *J. Chem. Phys.* **2010**, *133*, 014101.
(84) Jones, G. J.; Robertazzi, A.; Platts, J. A. *J. Phys. Chem. B* **2013**, *117*, 3315−3322.
(85) Quiñonero, D.; Estarellas, C.; Frontera, A.; Deyà, P. M. *Chem. Phys. Lett.* **2011**, *508*, 144−148.
(86) Zhao, Y.; Truhlar, D. G. *J. Phys. Chem. A* **2004**, *108*, 6908.
(87) *Computational Chemistry Comparison and Benchmark Database*. Release 16a; National Institute of Standards and Technology: 2013.
(88) Galbraith, J. M.; Schaefer, H. F. *J. Chem. Phys.* **1996**, *105*, 862−864.
(89) Rösch, N.; Trickey, S. B. *J. Chem. Phys.* **1997**, *106*, 8940−8941.
(90) Jensen, F. *J. Chem. Theory Comput.* **2010**, *6*, 2726.
(91) Lee, D.; Furche, F.; Burke, K. *J. Phys. Chem. Lett.* **2010**, *1*, 2124.
(92) Ruzsinszky, A.; Perdew, J. P.; Csonka, G. I.; Vydrov, O.; Scuseria, G. E. *J. Chem. Phys.* **2006**, *125*, 194112.
(93) Rienstra-Kiracofe, J. C.; Tschumper, G. S.; Schaefer, H. F.; Nandi, S.; Ellison, G. B. *Chem. Rev.* **2002**, *102*, 231−282.